

Qinghua Meng · Zhenqing Wang

Theoretical analysis of interfacial debonding and fiber pull-out in fiber-reinforced polymer-matrix composites

Received: 2 October 2014 / Accepted: 30 January 2015 / Published online: 14 February 2015
© Springer-Verlag Berlin Heidelberg 2015

Abstract A theoretical model is proposed to predict the interfacial debonding length and fiber pull-out length in fiber-reinforced polymer-matrix composites. The stress and displacement fields of fiber and matrix are derived considering the dual phase region model, and the relation between the pull-out length and debonding length of fiber is obtained. The interface debonding criterion is given based on the energy release rate relation in an interface debonding process. The formulas are applied in glass fiber-reinforced epoxy composites to demonstrate the newly theoretical model. The theoretical predictions of present model agree well with the experimental results. Several parameters studies are performed to analyze the debonding length and the pull-out length of fiber in glass fiber-reinforced epoxy composites.

Keywords Fiber-reinforced composites · Polymer-matrix composites · Interfacial debonding · Fiber pull-out · Theoretical analysis

1 Introduction

The interface between fiber and matrix in the fiber-reinforced polymer-matrix composites plays a major role in determining the mechanical properties of composites. The fiber pull-out test has been well accepted as one of the most popular and reliable test methods developed as a means of evaluating interfacial properties in the fiber-reinforced composites. Some experimental studies have shown that when a crack propagates through a matrix containing fibers, the fracture energies are absorbed by the failure mechanisms such as matrix cracking, interfacial debonding between fiber and matrix, post-debonding friction, fiber pull-out, fiber fracture, stress redistribution, among which the interfacial debonding and frictional sliding during fiber pull-out provide major contributions to the fracture toughness of most fiber-reinforced composites with polymer-based matrices [1].

The stress transfer through interface between fiber and matrix is an important problem which critically controls the mechanical properties of fiber-reinforced polymer-matrix composites under various loading conditions. The shear-lag model originally proposed by Cox [2] provides a good evaluation of the stresses in the fiber transferred from the matrix across the interface. Several shear-lag models were further developed to study the stress transfer in conventional fiber-reinforced composites [3–7] and carbon nanotube-reinforced polymer-matrix composites [8,9]. The effects of interphase on the stress transfer of the fiber- or carbon nanotube-reinforced polymer-matrix composites based on the three-phase shear-lag model including an interphase [10–15]. Based on the classical shear-lag theory and the strain gradient theory, Toll [16] presented a second order shear-lag theory for elastic aligned short-fiber-reinforced composites.

The interfacial debonding and fiber pull-out problem have received much attention in the past decades. There are two major approaches on the theoretical study of this problem: One is based on the maximum shear

Q. Meng (✉) · Z. Wang
College of Aerospace and Civil Engineering, Harbin Engineering University, Harbin 150001, China
Tel.: +86-451-82589364
E-mail: mengqinghua@hrbeu.edu.cn

stress criterion where the interfacial debonding occurs when the interfacial shear stress induced by loading reaches up to the interfacial shear strength. This approach is typified by the early work of Lawrence [17], Aveston and Kelly [18], Takaku and Arridge [19] and Hsueh [20] based on the shear-lag model. The other is based upon the critical energy release rate criterion of fracture mechanics where the debonding region is regarded as an interfacial crack and its propagation is dependent on the energy balance in terms of the interfacial fracture energy [21–33]. Hsueh and Becher [34] derived the relationship between the interfacial shear strength and the interfacial debonding energy using an effective circumferential defect at the interface, which is defined to account for the stress intensity due to the presence of the fiber in the matrix and the fiber pull-out geometry. Based on an interface constitutive equation, which is a bilinear elastic-softening relation between interface traction and fiber displacement, an analytical solution was performed for the interfacial debonding and fiber pull-out problem by Schreyer and Peffer [35]. Pavia et al. [36] extended the classical shear-lag model to predict the matrix cracking strength in a hybrid brittle-matrix composites containing both microscale and nanoscale fibers.

Frictional sliding of interface between fiber and matrix is an important problem, and its correct characterization remains an open issue. Theoretical models have usually assumed two characterization of sliding friction: A constant friction stress over all portions of the interface experiencing compressive normal stress [37–40], and Coulomb friction law which is caused by a friction coefficient and the normal stress across the interface [22,26,29,41]. Furthermore, considering both cases of constant friction and Coulomb friction, Hutchinson and Jensen [42] and Huang and Liu [43] studied the interfacial debonding and the fiber pull-out in the fiber-reinforced composites. The energy release rate of the interfacial crack is one of the most significant micromechanical parameters, and several theoretical models have been established for characterizing the interfacial fracture behavior. Chua and Piggott [44] and Piggott [45] studied the fiber pull-out test and obtained an expression for the interfacial fracture energy release rate. Budinasky et al. [22] developed an energy release rate relation which is dependent on the interfacial debonding length. Gao et al. [26] presented an energy release rate solution without considering the axial thermal stress of fiber and matrix. Sigl and Evans [41] derived an energy release rate expression in the form of a linear function of the debond length. Hutchinson and Jensen [42] obtained a steady-state energy release rate for interfacial debonding, which is not associated with the debonding length and the interfacial frictional stress. Other forms of the energy release rate with various levels of approximation have also been given [31,37,46–50].

To date, many studies have been carried out on the issues related to fiber debonding and pull-out in the fiber-reinforced composites, but theoretical prediction on the length of fiber debonding and pull-out is still very limited. Based on a fiber debonding criterion, Gao [37] and Gao et al. [26] presented a relation between fiber pull-out length and debonding load. Li et al. [30] derived an expression of the debonding length from energy considerations and using concepts of fracture mechanics. Hutchinson and Jensen [42] obtained an approximate result of the fiber debonding length and pull-out length within the framework of fracture mechanics and considering the interfacial friction. Kerans and Parthasarathy [28] yielded the expressions of the debonding length and pull-out length in terms of the external load for the fiber pull-out test. The interfacial debonding and fiber pull-out occur concurrently in the damage process of composites, but most theoretical researches only obtained one of interfacial debonding length and fiber pull-out length. Moreover, the interfacial debonding and fiber pull-out are influenced by loads, load increments and interfacial sliding. Therefore, in this paper, we propose a theoretical model to predict the interfacial debonding length and fiber pull-out length in fiber-reinforced composites, and study the effects of several parameters. The stress field and displacement field of fiber and matrix are obtained using the dual phase region model, and the interfacial debonding length is given by energy release rate criterion of interfacial debonding developed.

The rest of this paper is organized as follows: In Sect. 2, the failure mechanism of interfacial debonding in fiber-reinforced composites is described. The stress and displacement fields of fiber and matrix are derived, and the relation between the pull-out length and debonding length of fiber is obtained in Sect. 3. Energy release rate criterion for the interfacial debonding is given in Sect. 4. In Sect. 5, the parameters studies of theoretical model are carried out for a glass fiber-reinforced epoxy composites. Finally, Sect. 6 provides the concluding remarks.

2 Failure mechanisms of interfacial debonding

Consider a composite of unidirectional continuous fibers aligned parallel to the axis of applied load, as shown in Fig. 1. For the fiber-reinforced polymer-matrix composites under loads, the failure process generally starts

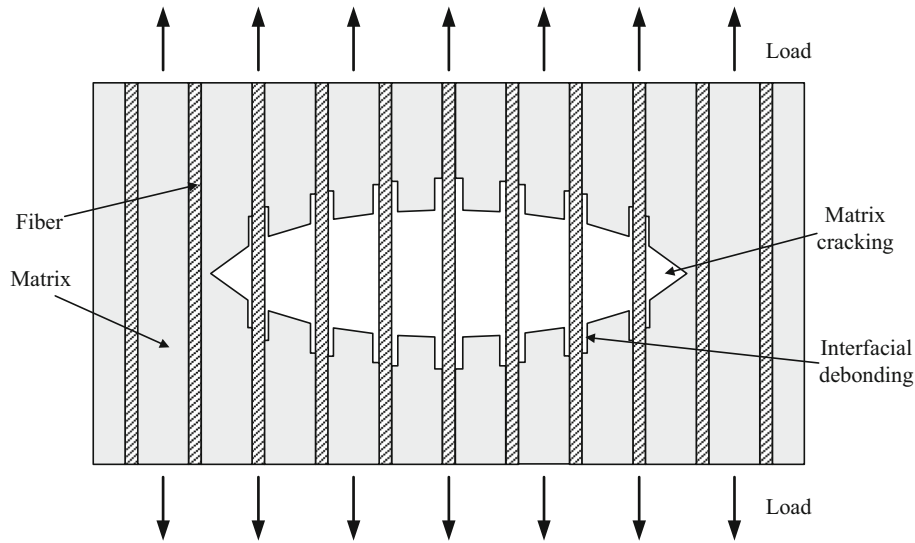


Fig. 1 Schematic of the interface debonding and matrix cracking in fiber-reinforced polymer composites

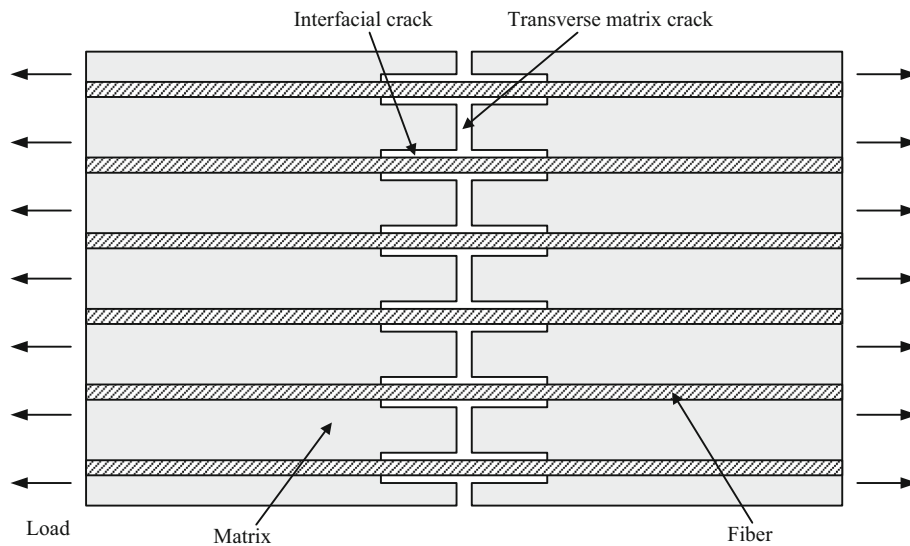


Fig. 2 Schematic of the post-cracking state of fiber-reinforced polymer-matrix composites under a uniform applied load

from the matrix cracking. The matrix cracking has initiated, while the fiber may still be intact, and the composite materials can continue to bear additional loads until the fracture strength of interface between fiber and matrix reaches up to the critical value. When the size of the matrix cracking is large enough and the external load reaches a certain critical value, the interfacial debonding will occur near the matrix cracking, and the interface protrudes to certain extent that enabled the crack to open. As the extent of these failures and the deformation of fibers along its length increase, the fibers are pulled out gradually. During fiber pull-out, residual clamping stresses due to matrix shrinkage on to the fiber during manufacture often exist at the interface and result in interfacial sliding for the debonding interface, which also continue to provide the load transfer between fiber and matrix. Therefore, after initial interfacial debonding, further interfacial debonding requires the applied stress to overcome the interfacial sliding stress of the debonding interface, and the bonding strength at the bonding interface. Actually, the interfacial debonding process is always accompanied by interfacial sliding and crack opening. The post-cracking state of fiber-reinforced polymer-matrix composites is shown in Fig. 2. Consequently, interface strength, interfacial sliding stress, debonding length and crack opening or pull-out length become the major effect factors on the micromechanical properties of fiber-reinforced composites.

3 Stress and displacement fields of fiber and matrix

According to Fig. 2, a simplified single-fiber pull-out model is considered, as shown in Fig. 3, where a fiber (of radius a) is embedded at the center of a coaxial cylindrical shell of matrix (of an outer radius b) with the fiber volume fraction

$$V_f = \frac{a^2}{b^2} \quad (1)$$

Then, the matrix volume fraction and the elastic modulus of the composite material are given by

$$V_m = 1 - V_f \quad (2)$$

$$E = E_m V_m + E_f V_f \quad (3)$$

where the subscripts f and m denote the fiber and the matrix, respectively. In this model, the fiber and the matrix are assumed to be elastic and isotropic. The embedded fiber length is L , and the initial partial debonding length is l from the free fiber end. Let the x direction be parallel to the fiber axis, and the matrix is fixed at one end ($x = L$), while a tensile stress is applied to the other end ($x = 0$) of the embedded fiber. The applied stress is assumed to be parallel to the fiber axis, and the applied stress for fiber and matrix at $x = 0$ is

$$\sigma_f = \frac{\sigma}{V_f} \quad (4a)$$

$$\sigma_m = 0 \quad (4b)$$

In the single-fiber pull-out test [19], the composite is fixed at one end and a tensile stress is applied at the other end of the embedded fiber at a constant displacement rate in the axial direction. Let u denote the applied constant displacement, the axial stress at $x = 0$ is

$$\sigma_f = \frac{u}{l} E_f \quad (5)$$

where l is the debonding length of fiber. For a given applied axial force P on the free end of the fiber, the axial stress at $x = 0$ is

$$\sigma_f = \frac{P}{\pi a^2} \quad (6)$$

The governing equations for the axis symmetric problem [51], in a displacement formulation and in terms of the polar coordinates (r, θ, x) , include the equilibrium equations (in the absence of body forces) are

$$\frac{\partial \sigma_{rr}}{\partial r} + \frac{\partial \tau_{rx}}{\partial x} + \frac{\sigma_{rr} - \sigma_{\theta\theta}}{r} = 0 \quad (7a)$$

$$\frac{\partial \tau_{rx}}{\partial r} + \frac{\partial \sigma_{xx}}{\partial x} + \frac{\tau_{rx}}{r} = 0 \quad (7b)$$

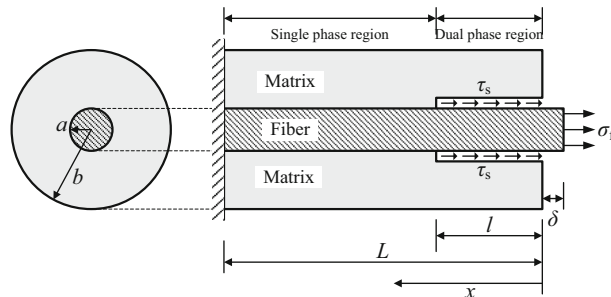


Fig. 3 Fiber pull-out model (or shear-lag model) of fiber-reinforced composites

The geometrical equations are

$$\varepsilon_{rr} = \frac{\partial w}{\partial r} \quad (8a)$$

$$\varepsilon_{\theta\theta} = \frac{w}{r} \quad (8b)$$

$$\varepsilon_{xx} = \frac{\partial u}{\partial x} \quad (8c)$$

$$\gamma_{rx} = \frac{\partial w}{\partial x} + \frac{\partial u}{\partial r} \quad (8d)$$

The constitutive equations are

$$\varepsilon_{rr} = \frac{\sigma_{rr} - v(\sigma_{\theta\theta} + \sigma_{xx})}{E} \quad (9a)$$

$$\varepsilon_{\theta\theta} = \frac{\sigma_{\theta\theta} - v(\sigma_{xx} + \sigma_{rr})}{E} \quad (9b)$$

$$\varepsilon_{xx} = \frac{\sigma_{xx} - v(\sigma_{rr} + \sigma_{\theta\theta})}{E} \quad (9c)$$

$$\gamma_{rx} = \frac{\tau_{rx}}{G} \quad (9d)$$

where σ_{rr} , $\sigma_{r\theta}$, σ_{xx} and τ_{rx} are stress components, ε_{rr} , $\varepsilon_{r\theta}$, ε_{xx} and γ_{rx} are strain components, w and u are the radial and axial displacement components, and E , v and G are the elastic modulus, Poisson's ratio and shear modulus of the material, respectively.

According to Gao [39], the debonding region defined by $0 \leq x \leq l$, is called dual displacement region or dual phase region in which the relative frictional slipping occurs along the interface. The undebonding region is called the single phase region. From the perspective of micromechanics, whether the dual phase or the single phase region, the real distributions of stress, strain and displacement are very complicated, we thus only consider the average value of each quantity. The initial residual stresses, the Poisson effects and the stress components in the radial directions are neglected since they are small compared to the axial stress component [6]. Let u_f and u_m denote the average displacements for fiber and matrix, respectively, then the relationships of displacements and axial stresses are given by

$$\sigma_f(x) = E_f \frac{\partial u_f(x)}{\partial x} \quad (10)$$

$$\sigma_m(x) = E_m \frac{\partial u_m(x)}{\partial x} \quad (11)$$

Consider the equilibrium of the axial force acting on the element of length dx in the debonding fiber and matrix shown in Fig. 4, we can have the following differential equation relating the rate of change of normal stress σ_f and σ_m along the x -axis and the interfacial sliding stress

$$\frac{\partial \sigma_f(x)}{\partial x} = -\frac{2}{a} \tau_s \quad (12)$$

$$\frac{\partial \sigma_m(x)}{\partial x} = \frac{2a}{b^2 - a^2} \tau_s = \frac{2V_f}{aV_m} \tau_s \quad (13)$$

where τ_s is the interface sliding stress between fiber and matrix, and the negative sign denotes that the direction of σ_f is opposite to that of σ_m . Equations (12) and (13) indicate the stress transfer between fiber and matrix in the debonding region.

The model is further simplified by concentrating all of the axial stress-carrying area, and assuming that the fiber and matrix supports only shear stresses [22]. The equilibrium and constitutive relations can be simplified to

$$\frac{\partial \tau_{rx}}{\partial r} + \frac{\tau_{rx}}{r} = 0 \quad (14)$$

$$\tau_{rx} = G \frac{\partial u}{\partial r} \quad (15)$$

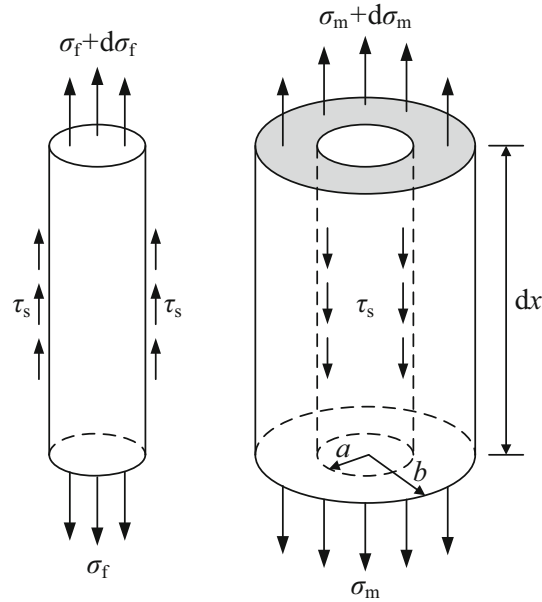


Fig. 4 Stresses acting on fiber and matrix of element in the debonding region

By solving (14) and taking into account the following stress boundary conditions

$$\tau_f(a, x) = \tau_s \quad (16a)$$

$$\tau_m(a, x) = \tau_s \quad (16b)$$

$$\tau_m(b, x) = 0 \quad (16c)$$

One can express the shear stresses distribution in fiber and matrix as

$$\tau_f(r, x) = \frac{a}{r} \tau_s \quad (0 < r \leq a) \quad (17)$$

$$\tau_m(r, x) = \frac{(b^2 - r^2)a}{(b^2 - a^2)r} \tau_s \quad (a \leq r \leq b) \quad (18)$$

Substituting Eqs. (17) and (18) into Eq. (15), and integrating from a to r for fiber and matrix, one gets

$$u_f(r, x) = u_f(a, x) + \tau_s \frac{a}{G_f} \ln \frac{r}{a} \quad (0 < r \leq a) \quad (19)$$

$$u_m(r, x) = u_m(a, x) + \tau_s \frac{\frac{a(a^2 - r^2)}{2} + ab^2 \ln \left(\frac{r}{a}\right)}{G_m(b^2 - a^2)} \quad (a \leq r \leq b) \quad (20)$$

where G_f and G_m are the shear modulus of fiber and matrix, respectively.

For the dual phase region, the deformation process is the superposition of two processes, the first is the deformation of single phase material without debonding, and the second is the interfacial debonding accompanied by the frictional slip [39]. If the displacements of the two processes are denoted by \hat{u} and \check{u} , then

$$u_f(x) = \hat{u}(x) + \check{u}_f(x) \quad (21a)$$

$$u_m(x) = \hat{u}(x) + \check{u}_m(x) \quad (21b)$$

Note that in the interfacial frictional slip process, the displacements \check{u}_f and \check{u}_m should be a self-equilibrating stress relation,

$$\frac{\partial \check{u}_f(x)}{\partial x} V_f E_f + \frac{\partial \check{u}_m(x)}{\partial x} V_m E_m = 0 \quad (22)$$

Then, the following relation can be given by

$$\tilde{u}_f(x) = \frac{V_m E_m}{E} \tilde{u}(x) \quad (23a)$$

$$\tilde{u}_m(x) = -\frac{V_f E_f}{E} \tilde{u}(x) \quad (23b)$$

Substituting Eq. (23) into Eq. (21), we have

$$\hat{u}(x) = \frac{V_f E_f}{E} u_f(x) + \frac{V_m E_m}{E} u_m(x) \quad (24a)$$

$$\check{u}(x) = u_f(x) - u_m(x) \quad (24b)$$

To determine the stress relation, assume that

$$\hat{\sigma}(x) = E \frac{\partial \hat{u}(x)}{\partial x} \quad (25a)$$

$$\check{\sigma}(x) = E \frac{\partial \check{u}(x)}{\partial x} \quad (25b)$$

Substituting Eqs. (21), (23) and (25) into Eqs. (10) and (11), we have

$$\sigma_f(x) = \frac{E_f}{E} \hat{\sigma}(x) + \frac{E_f}{E(1+\alpha)} \check{\sigma}(x) \quad (26a)$$

$$\sigma_m(x) = \frac{E_m}{E} \hat{\sigma}(x) - \frac{E_m \alpha}{E(1+\alpha)} \check{\sigma}(x) \quad (26b)$$

where

$$\alpha = \frac{V_f E_f}{V_m E_m} \quad (27)$$

Combination of Eqs. (12), (13) and (26), one gets

$$\frac{\partial \hat{\sigma}(x)}{\partial x} = 0 \quad (28a)$$

$$\frac{\partial \check{\sigma}(x)}{\partial x} = -\frac{2E(1+\alpha)}{aE_f} \tau_s \quad (28b)$$

For the single phase region ($l \leq x \leq L$), since the displacement at the interface between fiber and matrix ($r = a$) is continuous (perfect bonding), we have

$$u_f(x) = u_m(x) = \frac{\sigma}{E}(L-x) \quad (l \leq x \leq L) \quad (29)$$

The total axial stresses satisfy

$$V_f \sigma_f(x) + V_m \sigma_m(x) = \sigma \quad (l \leq x \leq L) \quad (30)$$

The stress transfer and stress distribution in the single phase region (full bonding region) have been extensively studied by Nairn [5], Fu et al. [6] and Qing [7]. No more about this will be mentioned here since it is not our main focus.

Based on the above analysis, the stress and displacement boundary conditions of the dual phase region are given by

$$\sigma_f(0) = \frac{\sigma}{V_f}, \sigma_m(0) = 0 \quad \text{at } x = 0 \quad (31)$$

$$u_f(l) = u_m(l) = \frac{\sigma}{E}(L-l) \quad \text{at } x = l \quad (32)$$

Substituting Eqs. (31) and (32) into Eqs. (24) and (26), the boundary conditions become

$$\hat{u}(l) = \frac{\sigma}{E}(L-l), \quad \hat{\sigma}(0) = \sigma, \quad (33)$$

$$\check{u}(l) = 0, \quad \check{\sigma}(0) = \frac{1+\alpha}{\alpha}\sigma, \quad (34)$$

Integrating of Eqs. (25a) and (28a), and considering the boundary condition (33), we have

$$\hat{\sigma}(x) = \sigma \quad (35)$$

$$\hat{u}(x) = \frac{\sigma}{E}(L-2l+x) \quad (36)$$

Similarly, Integrating of Eqs. (25b) and (28b), and taking into account the boundary condition (34), one gets

$$\check{\sigma}(x) = \frac{1+\alpha}{\alpha}\sigma - \frac{2E(1+\alpha)\tau_s}{aE_f}x \quad (37)$$

$$\check{u}(x) = \frac{(1+\alpha)\sigma}{\alpha E}(x-l) + \frac{(1+\alpha)\tau_s}{aE_f}(l^2-x^2) \quad (38)$$

Substituting Eqs. (35), (36), (37) and (38) into Eqs. (21), (23) and (26), the following stress and displacement fields can be obtained

$$\sigma_f(x) = \frac{(1+\alpha)E_f}{\alpha E}\sigma - \frac{2\tau_s}{a}x \quad (39a)$$

$$\sigma_m(x) = \frac{2V_f\tau_s}{aV_m}x \quad (39b)$$

$$\check{u}_f(x) = \frac{\sigma}{\alpha E}(x-l) + \frac{\tau_s}{aE_f}(l^2-x^2) \quad (40a)$$

$$\check{u}_m(x) = \frac{\sigma}{E}(l-x) + \frac{\alpha\tau_s}{aE_f}(x^2-l^2) \quad (40b)$$

$$u_f(x) = \frac{\sigma}{\alpha E}[L-(2\alpha+1)l+(\alpha+1)x] + \frac{\tau_s}{aE_f}(l^2-x^2) \quad (41a)$$

$$u_m(x) = \frac{\sigma}{E}(L-l) + \frac{\alpha\tau_s}{aE_f}(x^2-l^2) \quad (41b)$$

Then, combination of Eqs. (39a) and (39b), integrating from 0 to l for the debonding interface, the pull-out length can be given by

$$\delta = \int_0^l \left(\frac{\sigma_f(x)}{E_f} - \frac{\sigma_m(x)}{E_m} \right) dx = \frac{(1+\alpha)\sigma}{\alpha E}l - \frac{(1+\alpha)\tau_s}{aE_f}l^2 \quad (42)$$

Equation (42) is similar to the result obtained by the condition of energy balance [38]. According to Eqs. (38) and (42), we have

$$\delta = -\check{u}(0) \quad (43)$$

where the negative sign describes the assumption that the direction of fiber pull-out is opposite to the positive direction of axis, and Eq. (43) shows that the pull-out length is equivalent to the relative displacement between fiber and matrix.

4 Energy release rate criterion for interfacial debonding

The interfacial debonding of fiber-reinforced composite may be regarded as a crack propagation process along the interface between fiber and matrix. For a prestressed elastic body under constant additional load, a general relation is that crack propagation and opening is associated with the loss in potential energy and sliding occurred along internal interfaces. These relations will be applied in the steady-state crack growth calculations as follows.

Consider an elastic body Ω contains a steadily growing crack which possesses the interface sliding under loading, as shown in Fig. 5. In the initial state (1), the external vector tractions T is applied on the surface S_T , and the sliding traction τ is assumed on the crack surface S_C . The body contains an initial tensor stress distribution σ_1 , initial displacement u_1 and initial strain ε_1 . The body contains opening crack that is characterized by l_0 , as well as the internal surface in which sliding has occurred. With no change in T , the body further becomes the state (2), in which the length of crack becomes l , and the body now contains the stress σ_2 , displacement u_2 and strain ε_2 . The interface sliding stress τ_s always exists to resist the relative sliding along the crack surface S_C . Then, the total potential energy of the elastic body in each case can be given by

$$\pi_1 = \frac{1}{2} \int_{\Omega} \sigma_1 : \varepsilon_1 d\Omega - \int_{S_T} T \cdot u_1 dS \tag{44}$$

$$\pi_2 = \frac{1}{2} \int_{\Omega} \sigma_2 : \varepsilon_2 d\Omega - \int_{S_T} T \cdot u_2 dS \tag{45}$$

Further, considering $\varepsilon_1 : \sigma_2 = \varepsilon_2 : \sigma_1$, the released energy may be written as

$$\pi_2 - \pi_1 = \frac{1}{2} \int_{\Omega} (\sigma_1 + \sigma_2) : (\varepsilon_2 - \varepsilon_1) d\Omega - \int_{S_T} T \cdot (u_2 - u_1) dS \tag{46}$$

Since the state (2) is an equilibrium state with the sliding stress τ_s on the crack surface and the external load T , by the principle of virtual work we have

$$\int_{\Omega} \sigma_2 : (\varepsilon_2 - \varepsilon_1) d\Omega = \int_{S_T} T \cdot (u_2 - u_1) dS + \int_{S_C} \tau_s \cdot s dS \tag{47}$$

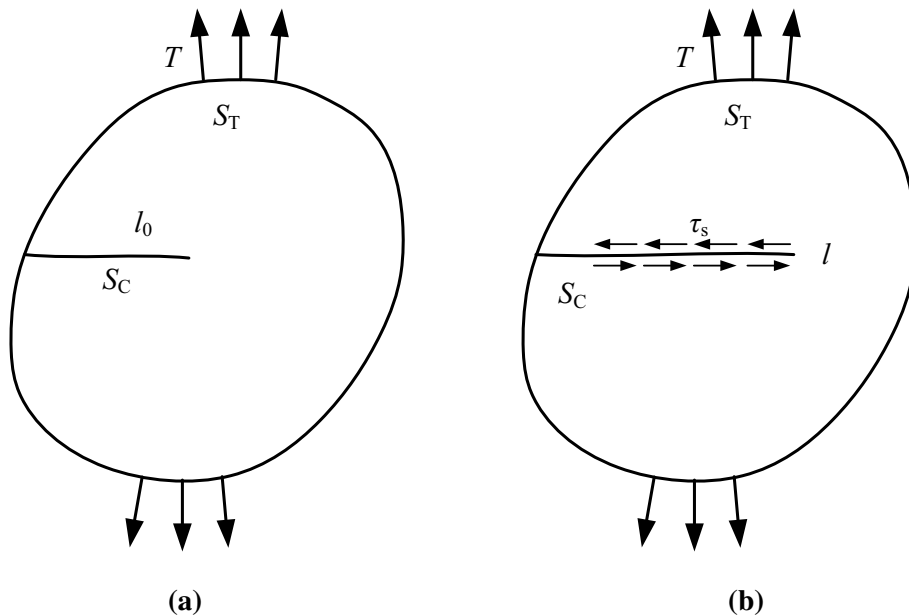


Fig. 5 Two states of crack growth in material with external loads and interface sliding: **a** state (1); **b** state (2)

where s is the magnitude of the relative slip on crack surface S_C . Then the combination of Eqs. (46) and (47), one gets

$$\pi_2 - \pi_1 = \frac{1}{2} \int_{\Omega} (\sigma_2 - \sigma_1) : (\varepsilon_2 - \varepsilon_1) d\Omega + \int_{S_C} \tau_s \cdot s dS \quad (48)$$

If we assume further that U_F is the friction dissipation energy by friction with sliding τ_s on the internal surface, then

$$\pi_2 - \pi_1 = \frac{1}{2} \int_{\Omega} (\sigma_2 - \sigma_1) : (\varepsilon_2 - \varepsilon_1) d\Omega + U_F \quad (49)$$

in which

$$U_F = \int_{S_C} \tau_s \cdot s dS \quad (50)$$

Let $\Delta\sigma$ and $\Delta\varepsilon$, denote the increment of stress and strain respectively, namely

$$\Delta\sigma = \sigma_2 - \sigma_1, \quad \Delta\varepsilon = \varepsilon_2 - \varepsilon_1 \quad (51)$$

Hence, Eq. (49) can be written as

$$\pi_2 - \pi_1 = \frac{1}{2} \int_{\Omega} \Delta\sigma : \Delta\varepsilon d\Omega + U_F \quad (52)$$

According to the Eq. (52), the potential energy release rate G , which is equivalent to the differential elastic strain energy stored in the constituents with respect to the incremental debonding length for the per unit thickness body, can be expressed as

$$G = \frac{\partial(\pi_2 - \pi_1)}{\partial l} = \frac{1}{2} \frac{\partial}{\partial l} \left(\int_{\Omega} \Delta\sigma : \Delta\varepsilon \right) d\Omega + \frac{\partial U_F}{\partial l} \quad (53)$$

For a unit debonding interface in the fiber-reinforced composite, the increment of surface area in per debonding fiber is $2\pi al$, where l is the debonding length, and the total release energy for such an interface is $2\pi alG_C$, where G_C is the critical energy release rate for the debonding interface between fiber and matrix. Then, we only consider an interfacial debonding process so that the energy release rate G must be balanced by the sum of the frictional energy dissipation rate and the energy release rate of the debonding interface. Hence, we have the following relation

$$\frac{1}{2} \frac{\partial}{\partial l} \left(\int_{\Omega} \Delta\sigma : \Delta\varepsilon d\Omega \right) = 2\pi aG_C \quad (54)$$

Equation (54) shows that the differential of increment of elastic strain energy with respect to the incremental debonding length is equivalent to the energy release rate of the interfacial debonding. We consider an interfacial debonding process where the interfacial debonding length changes from 0 to l , the release strain energy can be written as

$$\Delta U = \int_0^l \int_0^a \pi r \frac{V_f}{E_f} \sigma_f^2(x) dr dx + \int_0^l \int_a^b \pi r \frac{V_m}{E_m} \sigma_m^2(x) dr dx \quad (55)$$

Then, according to Eq. (54), we have

$$\frac{\partial}{\partial l} \left[\int_0^l \int_0^a r \frac{V_f}{E_f} \sigma_f^2(x) dr dx + \int_0^l \int_a^b r \frac{V_m}{E_m} \sigma_m^2(x) dr dx \right] = 2aG_C \quad (56)$$

Substituting Eq. (39) into Eq. (56), it can be obtained

$$\frac{(1 + \alpha)a}{4\alpha E} \Delta\sigma^2 - \frac{\Delta\sigma \tau_s l}{E_f} + \frac{(E_f + E_m)V_f}{aE_f E_m} \tau_s^2 l^2 = G_C \quad (57)$$

Equation (57) gives the energy release rate criterion for interfacial debonding in the fiber-reinforced composite, and the interfacial debonding length of fiber under loads can also be obtained using Eq. (57).

5 Results and discussions

In order to validate the theoretical model developed in the preceding section and study the effect of material parameters, the analyses are performed for a glass fiber-reinforced epoxy composites in this section. The mechanical properties of the fiber and matrix [52] are defined as: The Young's modulus of matrix is $E_m = 3$ GPa, the Young's modulus of glass fiber is $E_f = 70$ GPa, the radius of glass fiber is $a = 7$ μm , the ultimate strength of glass fiber is 1.65 GPa, the critical energy release rate of composites is $G_c = 50 \text{ J} \cdot \text{m}^{-2}$. The interface sliding stress τ_s will be assigned in the calculation process for lack of the required information.

For the interfacial debonding of composites, the initial debonding stress is also an important parameter. The initial debonding stress σ_d , which was obtained by Outwater and Murphy [53] based on the fracture energy, is described as

$$\sigma_d = 2 \left(\frac{E_f G_c}{a} \right)^{1/2} \quad (58)$$

For the glass fiber epoxy composites, the initial debonding stress approximately is 1.414 GPa, obtained by Eq. (58) and the corresponding material constants. In addition, the pull-out length of fiber in the fiber-reinforced composites can be obtained by Eq. (42). The relation between the pull-out length and debonding length of fiber for the glass fiber-reinforced composites is shown in Fig. 6 when $\sigma = 1.5$ GPa, $V_f = 15\%$, and the interface sliding stress $\tau_s = 0.5$ MPa. It can be seen that theoretical predictions have a reasonable agreement with the experimental results [52]. To study the effect of the material parameters, the pull-out lengths versus the load, the fiber volume fraction and the interface sliding stress in the glass fiber-reinforced epoxy composites are shown in Figs. 7, 8 and 9. It can be found that the pull-out length increases linearly with the increase in applied load, while the pull-out length decreases gradually with the increase in interface sliding stress, and the effect of load is larger than that of the interface stress when the other material parameters are given. Furthermore, the pull-out length decreases gradually and closes to a limit value as the fiber volume fraction increases at the same debonding length.

The debonding length of fiber in fiber-reinforced composites can be given by Eq. (57). For the given materials, the debonding length is mainly determined by the load increment. The debonding length versus load increment for the glass fiber-reinforced composites is shown in Fig. 10 when $V_f = 15\%$, and the interface sliding stress $\tau_s = 0.5$ MPa. It can be observed that with the increase in load increments, the debonding length of fiber shows a nonlinear increase trend. Furthermore, the debonding length versus fiber volume fraction and interface sliding stress for the various load increments in glass fiber-reinforced epoxy composites are plotted in Figs. 11 and 12. It can be seen that the debonding length of fiber shows a nonlinear decrease trend as the fiber volume fraction increases, and the debonding length also shows a decrease trend with the increasing of the interface sliding stress. This trend of debonding length has also been observed by Chiang [33] and this also verified our theoretical results.

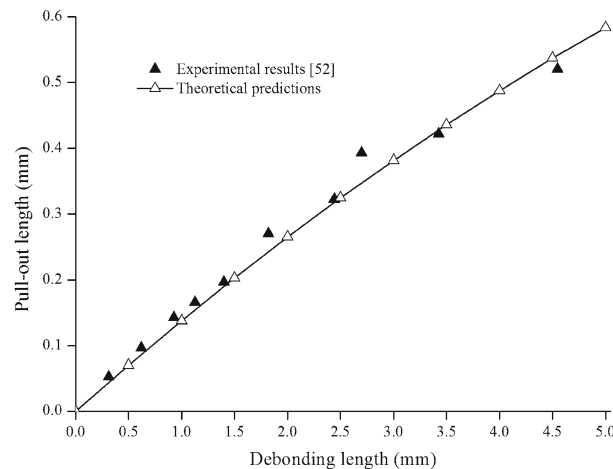


Fig. 6 Comparison between theoretical predictions and experimental results for relation of fiber pull-out length and debonding length [52] in glass fiber-reinforced epoxy composite

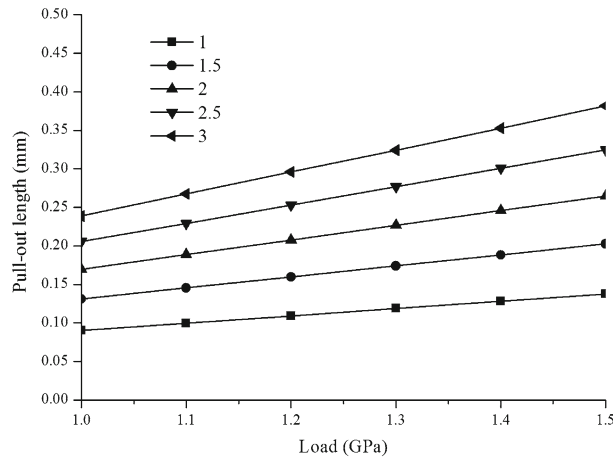


Fig. 7 Pull-out length versus applied load for the different debonding lengths (mm) in glass fiber-reinforced epoxy composites

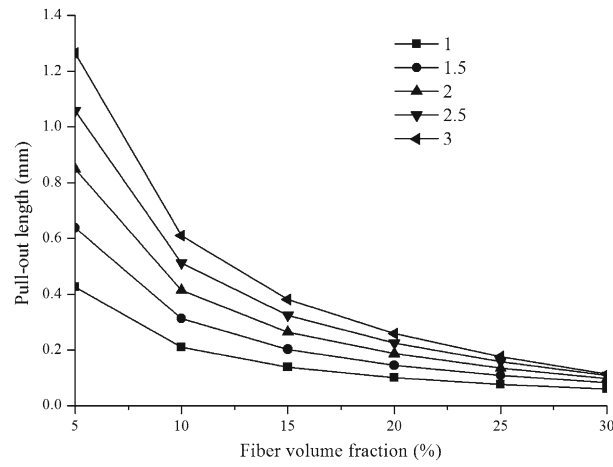


Fig. 8 Pull-out length versus fiber volume fraction for the different debonding lengths (mm) in glass fiber-reinforced epoxy composites

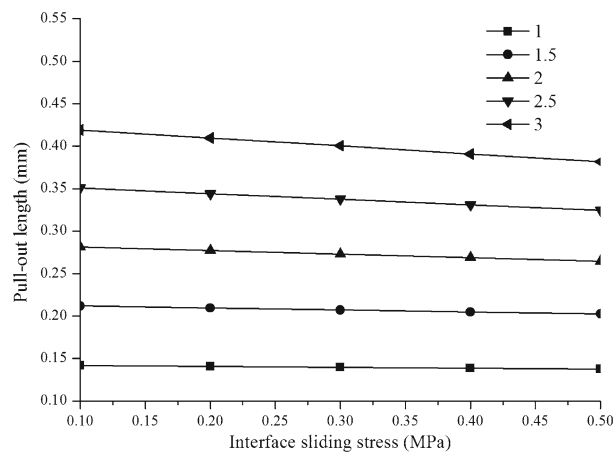


Fig. 9 Pull-out length versus interface sliding stress for the different debonding lengths (mm) in glass fiber-reinforced epoxy composites

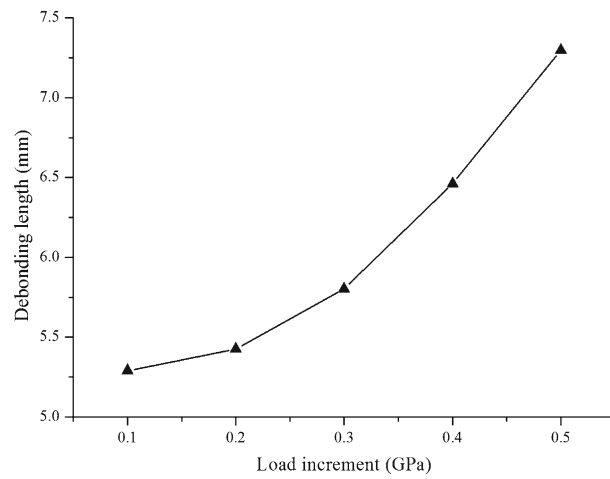


Fig. 10 The debonding length of fiber for the different load increments in glass fiber-reinforced epoxy composites with $V_f = 15\%$ and $\tau_s = 0.5$ MPa

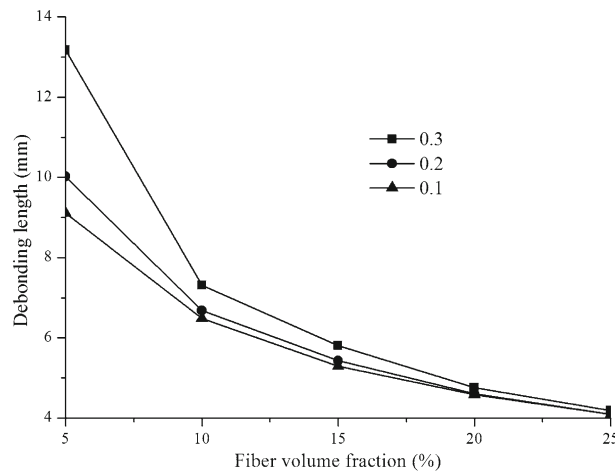


Fig. 11 Debonding length versus fiber volume fraction for various load increments (GPa) in glass fiber-reinforced epoxy composites

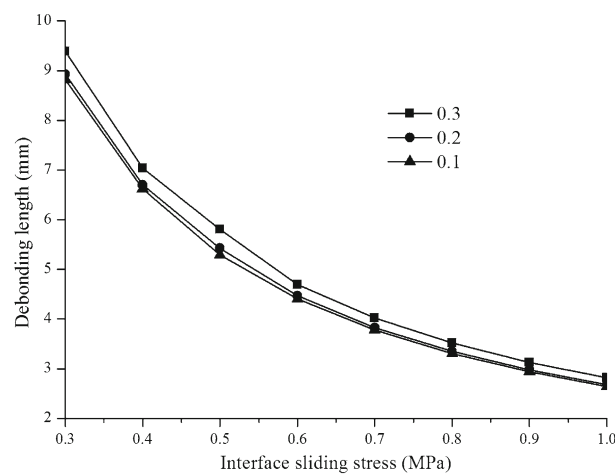


Fig. 12 Debonding length versus interface sliding stress for various load increments (GPa) in glass fiber-reinforced epoxy composites

6 Concluding remarks

A theoretical prediction of interfacial debonding and fiber pull-out process has been carried out in fiber-reinforced polymer-matrix composites. The interfacial debonding and fiber pull-out are considered simultaneously. Relation between the pull-out length and debonding length of fiber was obtained considering the dual phase region model. The interface debonding criterion was given based on the energy release rate relation in an interface debonding process.

The formulas were applied in glass fiber-reinforced epoxy composites to demonstrate the newly developed theoretical model. The theoretical predictions of present model agree well with the experimental results. Several parameters studies were presented to analyze the debonding length and the pull-out length of fiber in glass fiber-reinforced epoxy composites. The results showed that with the increase in applied load, the pull-out length of fiber increases linearly while the debonding length decreases gradually with the increase in interface sliding stress. The pull-out length of fiber decreases gradually as the fiber volume fraction increases at the same debonding length. The debonding length of fiber shows a nonlinear decrease trend with the increasing of the fiber volume fraction and interface sliding stress.

Actually, for a given fiber-reinforced composite material, first the interfacial debonding length of fiber under loads is obtained by Eq. (57), and then the pull-out length of fiber accompanied by the interfacial debonding can be given using Eq. (42). Note that many research works of debonding and pull-out problem have been carried out in the last several decades, but the measurement and analysis of the whole process are limited. Therefore, the understanding and measurement of the debonding and pull-out processes still need to perform further because they affect the fracture toughness of fiber-reinforced composites.

Acknowledgments This work is supported by the National Natural Science Foundation of China (11272096, 11472086) and the Research Fund for the Doctoral Program of Higher Education of China (20112304110015).

References

- Kim, J.K., Baillie, C., Mai, Y.W.: Interfacial debonding and fibre pull-out stresses Part I Critical comparison of existing theories with experiments. *J. Mater. Sci.* **27**, 3143–3154 (1991)
- Cox, H.L.: The elasticity and strength of paper and other fibrous materials. *Brit. J. Appl. Phys.* **3**, 72–79 (1952)
- McCartney, L.N.: New theoretical model of stress transfer between fibre and matrix in a uniaxially fibre-reinforced composite. *Proc. R. Soc. Lond. A* **425**, 215–244 (1989)
- Hsueh, C.H.: A modified analysis for stress transfer in fiber-reinforced composites with bonded fiber ends. *J. Mater. Sci.* **30**, 219–224 (1995)
- Nairn, J.A.: On the use of shear-lag methods for analysis of stress transfer in unidirectional composites. *Mech. Mater.* **26**, 63–80 (1997)
- Fu, S.Y., Yue, C.Y., Hu, X., Mai, Y.W.: Analyses of the micromechanics of stress transfer in single- and multi-fiber pull-out tests. *Compos. Sci. Technol.* **60**, 569–579 (2000)
- Qing, H.: A new theoretical model of the quasistatic single-fiber pullout problem: Analysis of stress field. *Mech. Mater.* **60**, 66–79 (2013)
- Gao, X.L., Li, K.: A shear-lag model for carbon nanotube-reinforced polymer composites. *Int. J. Solids Struct.* **42**, 1649–1667 (2005)
- Haque, A., Ramasetty, A.: Theoretical study of stress transfer in carbon nanotube reinforced polymer matrix composites. *Compos. Struct.* **71**, 68–77 (2005)
- Tsai, H.C., Arocho, A.M., Gause, L.W.: Prediction of fiber-matrix interphase properties and their influence on interface stress, displacement and fracture toughness of composite material. *Mater. Sci. Eng. A* **126**, 295–304 (1990)
- Monette, L., Anderson, M.P., Grest, G.S.: Effect of interphase modulus and cohesive energy on the critical aspect ratio in short-fibre composites. *J. Mater. Sci.* **28**, 79–99 (1993)
- Afonso, J.C., Ranalli, G.: Elastic properties of three-phase composites: analytical model based on the modified shear-lag model and the method of cells. *Compos. Sci. Technol.* **65**, 1264–1275 (2005)
- Zhang, J., He, C.: A three-phase cylindrical shear-lag model for carbon nanotube composites. *Acta Mech.* **196**, 33–54 (2008)
- Yao, Y., Chen, S.H., Chen, P.J.: The effect of a graded interphase on the mechanism of stress transfer in a fiber-reinforced composite. *Mech. Mater.* **58**, 35–54 (2013)
- Yao, Y., Chen, S.H.: The effects of fiber's surface roughness on the mechanical properties of fiber-reinforced polymer composites. *J. Compos. Mater.* **47**, 2909–2923 (2013)
- Toll, S.: Second order shear lag theory. *Compos. Sci. Technol.* **72**, 1313–1317 (2012)
- Lawrence, P.: Some theoretical considerations of fibre pull-out from an elastic matrix. *J. Mater. Sci.* **7**, 1–6 (1972)
- Aveston, J., Kelly, A.: Theory of multiple fracture of fibrous composites. *J. Mater. Sci.* **8**, 352–362 (1973)
- Takaku, A., Arridge, R.G.C.: The effect of interfacial radial and shear stress on fibre pull-out in composite materials. *J. Phys. D: Appl. Phys.* **6**, 2038–2047 (1973)
- Hsueh, C.H.: Interfacial debonding and fiber pull-out stresses of fiber-reinforced composites. *Mater. Sci. Eng. A* **123**, 1–11 (1990)

21. Gurney, C., Hunt, J.: Quasi-static crack propagation. *Proc. R. Soc. Lond. A* **299**, 508–524 (1967)
22. Budinasky, B., Hutchinson, J.W., Evans, A.G.: Matrix fracture in fiber-reinforced ceramics. *J. Mech. Phys. Solids* **34**, 167–189 (1986)
23. Budiansky, B., Evans, A.G., Hutchinson, J.W.: Fiber-matrix debonding effects on cracking in aligned fiber ceramic composites. *Int. J. Solids Struct.* **32**, 315–328 (1995)
24. Stang, H., Shah, S.P.: Failure of fibre-reinforced composites by pull-out fracture. *J. Mater. Sci.* **21**, 953–957 (1986)
25. McCartney, L.N.: Mechanics of matrix cracking in brittle-matrix fibre-reinforced composites. *Proc. R. Soc. Lond. A* **409**, 329–350 (1987)
26. Gao, Y.C., Mai, Y.W., Cotterell, B.: Fracture of fiber-reinforced materials. *J. Appl. Math. Phys. (ZAMP)* **39**, 550–572 (1988)
27. Charalambides, P.G., Evans, A.G.: Debonding properties of residually stressed brittle-matrix composites. *J. Am. Ceram. Soc.* **72**, 746–753 (1989)
28. Kerans, R.J., Parthasarathy, T.A.: Theoretical analysis of the fiber pullout and pushout tests. *J. Am. Ceram. Soc.* **74**, 1585–1596 (1991)
29. Zhou, L.M., Kim, J.K., Mai, Y.W.: Interfacial debonding and fibre pull-out stresses Part II A new model based on the fracture mechanics approach. *J. Mater. Sci.* **27**, 3155–3166 (1992)
30. Li, S.H., Shah, S.P., Li, Z.J., Toshio, M.: Micromechanical analysis of multiple fracture and evaluation of debonding behavior for fiber-reinforced composites. *Int. J. Solids Struct.* **30**, 1429–1459 (1993)
31. Hsueh, C.H.: Interfacial debonding and fiber pull-out stresses of fiber-reinforced composites: VIII: The energy-based debonding criterion. *Mater. Sci. Eng. A* **159**, 65–72 (1992)
32. Hsueh, C.H.: An asymptotic approach for debonding at the fiber-matrix interface. *Mater. Sci. Eng. A* **174**, L17–L22 (1994)
33. Chiang, Y.C.: On fiber debonding and matrix cracking in fiber-reinforced ceramics. *Compos. Sci. Technol.* **61**, 1743–1756 (2001)
34. Hsueh, C.H., Becher, P.F.: Interfacial shear debonding problems in fiber-reinforced ceramic composites. *Acta Mater.* **46**, 3237–3245 (1998)
35. Schreyer, H.L., Peffer, A.: Fiber pullout based on a one-dimensional model of decohesion. *Mech. Mater.* **32**, 821–836 (2000)
36. Pavia, F., Letertre, A., Curtin, W.A.: Prediction of first matrix cracking in micro/nanohybrid brittle matrix composites. *Compos. Sci. Technol.* **70**, 916–921 (2010)
37. Gao, Y.C.: Debonding along the interface of composites. *Mech. Res. Comm.* **14**, 67–72 (1987)
38. Gao, Y.C.: Damage modeling of fiber-reinforced materials. *Theor. Appl. Fract. Mech.* **11**, 147–155 (1989)
39. Gao, Y.C.: Damage theory of fiber-reinforced materials. *Sci. China Ser. A* **32**, 953–961 (1989)
40. Chiang, Y.C., Wang, A.S.D., Chou, T.W.: On matrix cracking in fiber reinforced ceramics. *J. Mech. Phys. Solids* **41**, 1137–1154 (1993)
41. Sigl, L.S., Evans, A.G.: Effects of residual stress and frictional sliding on cracking and pull-out in brittle matrix composites. *Mech. Mater.* **8**, 1–12 (1989)
42. Hutchinson, J.W., Jensen, H.M.: Models of fiber debonding and pullout in brittle composites with friction. *Mech. Mater.* **9**, 139–163 (1990)
43. Huang, N.C., Liu, X.Y.: Debonding and fiber pull-out in reinforced composites. *Theor. Appl. Fract. Mech.* **21**, 157–176 (1994)
44. Chua, P.S., Piggot, M.R.: The glass fiber-polymer interface, I. Theoretical consideration for single fiber pull-out tests. *Compos. Sci. Technol.* **22**, 33–42 (1985)
45. Piggot, M.R.: Debonding and friction at fiber-polymer interfaces, I. Criteria for failure and sliding. *Compos. Sci. Technol.* **30**, 295–306 (1987)
46. Hsueh, C.H.: Crack-wake interfacial debonding criteria for fiber-reinforced ceramic composites. *Acta Mater.* **44**, 2211–2216 (1996)
47. Gao, Y.C., Zhou, L.M.: Energy release rate for interface debonding with prestress and friction. *Theor. Appl. Fract. Mech.* **32**, 203–207 (1999)
48. Zhang, S.Y.: A new model for the energy release rate of fiber/matrix interfacial fracture. *Compos. Sci. Technol.* **58**, 163–166 (1998)
49. Zhang, S.Y.: Debonding and cracking energy release rate of the fiber/matrix interface. *Compos. Sci. Technol.* **58**, 331–335 (1998)
50. Liu, Y.F., Kagawa, Y.: The energy release rate for an interfacial debond crack in a fiber pull-out model. *Compos. Sci. Technol.* **60**, 167–171 (2000)
51. Timoshenko, S.P., Goodier, J.N.: *Theory of Elasticity*, 3rd edn. McGraw-Hill, New York (1970)
52. Wells, J.K., Beaumont, P.W.R.: Debonding and pull-out processes in fibrous composites. *J. Mater. Sci.* **20**, 1275–1284 (1985)
53. Outwater, J.D., Murphy, M.C.: On the fracture energy of unidirectional laminates. 24th Annual Technical Conference on Composites (The Society of the Plastics Industry), New York (1969)